Molecular BioSystems

Accepted Manuscript

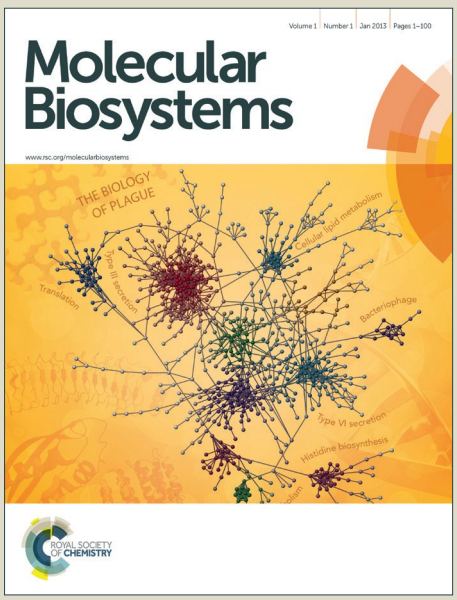

ROYAL SOCIETY OF CHEMISTRY

www.rsc.org/molecularbiosystems

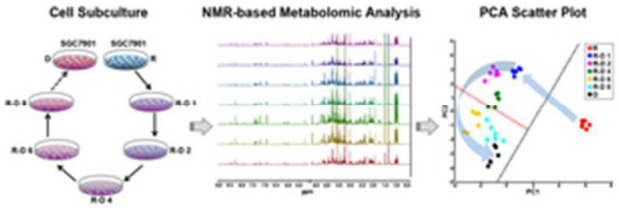

Textual abstract: Culture media significantly affect cellular metabolic profiling.
26x8mm (300 x 300 DPI)

Effects of Culture Media on Metabolic Profiling of Human Gastric Cancer Cell Line SGC7901

Zicheng Huang,[a, †] Wei Shao,[a, b, †] Jinping Gu,[a] Xiaomin Hu,[a] Yuanzhi Shi,[a] Wenqi Xu,[a] Caihua Huang,[c,*] and Donghai Lin[a,*]

[a] High-field NMR Research Center, College of Chemistry and Chemical Engineering, Xiamen University, Xiamen 361005, P. R. China

[b] Chenggong Hospital, Xiamen University, Xiamen 361005, China

[c] Department of Physical Education, Xiamen University of Technology, Xiamen 361005, China

Abstract

Cell culture metabolomics has demonstrated significant advantages in cancer research. However, its applications have been impeded by some influencing factors such as culture media, which could significantly affect cellular metabolic profiles and cause inaccuracy and unreliability for comparative metabolomic analysis of cells. To evaluate the effects of different culture media on cellular metabolic profiling, we performed NMR-based metabolomic analysis of human gastric cancer cell line SGC7901 cultured in both RPMI1640 and DMEM. We found that SGC7901 cultured in the two media exhibited distinct metabolic profiles with obviously different levels of discrepant metabolites, even though they showed almost the same cellular morphology and proliferation rate. When SGC7901 originally cultured in RPMI1640 were gradually acclimated in DMEM, both the metabolic profiles and most of the discrepant metabolite levels gradually converged toward those of the cells originally cultured in DMEM without significantly altered cell proliferation rates. However, several metabolite levels did not show the converging trends. Our results indicate that the effects of culture media on metabolic profiling must be carefully taken into account for comparative metabonomic analysis of cell lines. This work may be of benefit to the development of cell culture metabolomics.

Keywords: Metabolomics · culture medium · cancer cell line · metabolic profile

1. Introdction

Cell culture metabolomic analysis is a quantitative study of the full networks of cellular metabolism, offering the closest direct measurement of cellular physiological activities and abundant information about specific cell types under different conditions. It also provides global metabolic information, either independently or directly combined with other 'omics' analyses, and greatly aids other cell culture studies in the interpretation of various metabolic responses.[1-3] In the recent years, cell culture metabolomic analysis has been widely used for targeted treatment monitoring,[4, 5] diagnostic marker searching,[6-8] drug screening,[9] cell metabolic phenotype characterizing (such as growth and productivity).[10-12] Moreover, cell culture metabolomic analysis has also recently been exploited as novel and efficient approaches for cancer diagnosis and prognosis monitoring.[13] Furthermore, metabolic profiling of cell lines usually works as a prerequisite to more complicated metabolic analysis of tumor tissue or biopsy samples. In a previous work, Miroslava *et al* performed metabolic profiling of different glioblastoma lines and demonstrated that distinct subtypes of the cell lines were highly correlated with gene expression differences.[14]

In addition, cell culture metabolomic analysis is also employed to compare metabolic profiles among several types of cell lines aiming to clarify the metabolism of cultured cells themselves. As cell culture conditions have significant effects on cellular metabolism, homogeneity of culture conditions is thus required for the comparative metabolomic analysis. However, different types of cell lines usually have

their own optimum culture media, which would affect the results of the metabolomic analysis. It is well known that cellular metabolic profiles are extremely sensitive to various environmental factors, such as the used culture medium, the dissolved oxygen level in the culture medium, temperature, and so on.[13, 15] Among these factors, the culture medium is a crucial one influencing cell growth and survival, the expression of products and especially the metabolic profile,[16, 17] and thus exerts different biological effects on different type of the cells. So far, few work has been devoted to evaluate the effects of culture media on metabolic profiling of cell lines, which might lead to inaccurate and unreliable results. Hence, it is necessary to assess the effects of culture media on global metabolic profiles of cell lines. Furthermore, some metabolomic analyses were conducted on different types of cell lines cultured in different media, which might cause an obvious obstacle for interpreting and comparing the results of metabolomic analysis. In a previous work, Pratima *et al* delineated metabolic signatures of head and neck squamous cell carcinoma (HNSCC) cells from five different patients, and cultured them in Dulbecco's modified Eagle's medium.[18] In addition, they chose normal human oral keratinocytes (NHOK) cells for the comparison of the metabolic profiles, and cultured them in oral keratinocyte medium, which was distinctly different from the medium for culturing HNSCC cells. As different culture medium might have different effects on cellular metabolic profiles, it would be actually difficult to accurately compare the metabolic profiles of HNSCC and NHOK cells.

On the other hand, many cancer cell lines can usually be cultured in more than

one kind of media. It is not clear whether different cell lines could be acclimated to a same culture medium to eliminate the effects of culture media on metabolic profiling. Therefore, it is also indispensable to address the changes of metabolic profiles when cell lines are acclimated from one culture medium to another.

SGC7901 is a commercial human gastric cancer cell line with an optimal culture medium of RPMI1640, as suggested by the American Type Culture Collection (ATCC). In addition, SCG7901 can also be well cultured in DMEM, just as previously reported.[19, 20] Actually, both RPMI1640 and DMEM are common-used media for culturing cancer cell lines. In the present study, we cultured SGC7901 cells in both RPMI1640 and DMEM, and performed NMR-based metabolomic analysis to compare the cellular metabolic profiles. When SGC7901 cells originally cultured in RPMI1640 were gradually acclimated in the culture medium of DMEM, their metabolic signatures were monitored during the acclimation process. We found that both the metabolic profile and discrepant metabolite levels of SGC7901 cells cultured originally in RPMI1640 were distinctly different from those of the cells cultured originally in DMEM. Furthermore, the acclimation from RPMI1640 to DMEM could well eliminate the differences of both the metabolic profiles and most of the discrepant metabolite levels between the two media. However, the differences of several metabolite levels could not be mostly eliminated through multiple subcultures, which would lead to inaccurate and unreliable results of the metabolic analysis. Thus, the effects of the culture media on metabolic profiling must be carefully taken into account when performing metabolomic analysis on several types of cell lines cultured

in different culture media. This work may be beneficial to the development of cell culture metabolomic analysis and lay the foundation for finding small molecular based-maker of specific medium treated cancerous cells.

2. Methods

2.1 Cell culture

The human gastric cancer cell line SGC7901 was cultured in 10 cm cell culture dish in 5 ml of commercial culture medium RPMI1640 or DMEM (HyClone, USA), respectively. The components and corresponding concentrations in the two culture media are showed in Table S1. Media were supplemented with 10% (v/v) fetal bovine serum (PAA Laboratories, Cölbe, Germany), 100 U/ml penicillin and 100 μg/ml streptomycin. Cell culture was carried out at 37 °C in a humidified atmosphere of 5% (v/v) CO_2. Cells were harvested after 48 h culture, at around 5-10×10^6 cells, to allow detection of less abundant metabolites.

In the present work, SGC7901 cells originally cultured in RPMI1640 and DMEM were named as R group and D group, respectively. For gradual subculture, we changed the culture medium from RPMI1640 to DMEM. During the acclimation process, the SGC7901 cells after 1, 2, 4, 6, 8 times of subculture were indicated as R-D 1, R-D 2, R-D 4, R-D 6, R-D 8 groups, respectively. Six replicates were used for each cell group.

2.2 MTS cell proliferation assay

The cell proliferation rate was measured with CellTiter 96® AQ_{ueous} One Solution Cell Proliferation Assay Kit (Promega, USA) according to the recommendation of

manufacturer, by assessing the capacity of cells to reduce the 3-(4,5-dimethyl-thiazol-2-yl)-5-(3-carboxymethoxyphenyl)-2-(4-sulfophenyl)-2H-tet-razolium salt (MTS) to blue formazan which could be directly dissolved in culture medium. Cells cultured in RPMI1640 and DMEM were seeded at a density of 2×10^3 per well in 96-well plates. Equivalent volumes of vehicle culture media were treated as controls. After 48 h culture (just being consistent with the harvest time), 20 μl of MTS was added to each well containing 100 μl of culture medium, and then incubated in the dark at 37 °C for 3 h before measuring the absorbance of formazan at a wavelength of 490 nm on the microplate reader (BioTek, USA).

Morphological changes of SGC7901 were evaluated by inverted microscope after being cultured for 48 h. The phase contrast photographs were taken by inverted fluorescence microscope (Zeiss Axio Observer A1, Germany). Pictures were taken at random visual points after removing non-adherent cells.

2.3 Sample collection and preparation

Cell extracts were prepared using the pre-cooled methanol/chloroform/water system as previously described.[21] After the culture medium was removed from the culture dish, cells were quickly washed thrice with ice-cold PBS (pH 7.4) to remove medium components. The residual PBS was removed by vacuum suction. Cells were then immediately quenched by using 3 ml of HPLC grade methanol within seconds before being gently detached from the culture dish with a cell scraper (Costar, Mexico). The methanol solution containing the quenched cells was pipetted into a 15 ml polypropylene centrifuge tube. Then, 3 ml of HPLC grade chloroform and 2.5 ml of

ultrapure H_2O were added and mixed for extraction. After 30 min, the solution was centrifuged at 12,000 g for 15 min at 4 □ to separate two phase extracts. All the operations were conducted on the ice. Only the aqueous phase was lyophilized and subjected to NMR-based metabolomic analysis.

Lyophilized intracellular metabolite extracts were resuspended in 450 μl of D_2O and 50 μl of sodium phosphate buffer (1.5 M K_2HPO_4 / NaH_2PO_4, pH 7.4) including 0.1% sodium 3-(trimethylsilyl)propionate-2,2,3,3-d4 (TSP) and 0.2% NaN_3. D_2O was used for field frequency lock, and TSP provided the chemical shift reference (δ 0.00). All the samples were mixed uniformly and then centrifuged at 12,000 g for 15 min at 4 □. The supernatants were transferred into 5 mm NMR tubes for further measurement.

2.4 NMR measurements and data preprocessing

All NMR measurements were performed on a Bruker Avance □ 600 MHz spectrometer (Bruker BioSpin, Rheinstetten, Germany) at 298 K. One-dimensional ^1H spectra were obtained with the pulse sequence noesypr1d [RD-90°-t_1-90°-τ_m-90°-acq]. (BrukerBiospin pulse program library). Water suppression irradiation was applied during the relaxation delay (3 s) and the mixing time (τ_m) of 120 ms. A total of 128 FIDs were collected into 32,768 data points using a spectral width of 16 ppm with acquisition time of 1.64 s. Chemical shifts were calibrated by aligning the TSP signal at 0 ppm. Both phase and baseline corrections were carefully performed.

To aid resonance assignments of metabolites, several 2D ^1H-^1H spectra were acquired on selected samples, including J-resolved, COSY and TOCSY, using default

pulse sequences as provided by Bruker.

NMR spectral data were preprocessed using the MestReNova 6.1 software (Mestrelab Research S.L, Espain) with exponential apodization, global phase correction, Bernstein-Polynomial baseline correction, normalization using total spectral area as provided in the software. The integrals from the region of δ 5.23-4.68 were excluded to eliminate distorted baseline from residual water resonances in all spectra. The spectral region of δ 9.40-0.70 was binned by 0.002 ppm intervals for further statistical analysis. The integrals were normalized using the approach of probabilistic quotient normalization (PQN) to compensate for dilution-independent effects on spectral area in MatLab (Version 2011b, Math Works, USA).[22]

2.5 Metabolites identification

Metabolites identification was determined by using Chenomx NMR Suite (version 7.7, Chenomx Inc., Edmonton, Canada). TSP was used as a concentration reference. Further assignment confirmation was performed by a combination of the Human Metabolome Data Base (HMDB) (http://www.hmdb.ca/) and Biological Magnetic Resonance Data Bank (BMRB) (http://www.bmrb.wisc.edu/metabolomics/), as well as compared with relevant published references.

2.6 Statistical analysis

Multivariate data analysis was conducted in the SIMCA-P+ V12.0.1 software package (Umetrics, Umeå , Sweden). Normalized integral values were scaled by Pareto scaling. As an unsupervised approach, principal component analysis (PCA) in conjunction

with linear discriminant classification was performed for pattern recognition. Both hierarchical clustering analysis and K-means cluster analysis were used for further confirmation.[23] In hierarchical cluster analysis, each sample works as a separate cluster initially and the algorithm proceeds to combine them until all samples belong to one cluster. K-means clustering is a nonhierarchical clustering technique for creating k clusters such that the sum of squares from points to the assigned cluster centers is minimized. It begins by creating k random clusters, then calculates the mean of each cluster. If an observation is closer to the centroid of another cluster, then the observation is made a member of that cluster. This process is repeated until none of the observations are reassigned to a different cluster. In addition, both partial least-squares discriminant analysis (PLS-DA) and orthogonal partial least-squares discriminant analysis (OPLS-DA), were conducted to check grouping trends. These supervised approaches used class membership information to attempt maximum segregation among different classes of observations and built models that could be used to detect potential metabolites for discriminating among cell groups. The standard cross validation by random permutation test (999 cycles) was carried out to evaluate the robustness of the model. The extracted R2 and Q2 values reflected the explained variance and predictive capabilities, respectively.

To extract the discrepant metabolites significantly affecting the metabolic profiles of SGC7901 cultured in RPMI1640 and DMEM, a careful screening procedure was performed. First, significantly different variables were extracted from the S-plot in the OPLS-DA model. Among the data set, the mostly altered variables

were involved in s-plot generation. The variables with higher p and p(corr) values were the vital variables that had the greatest influence on cluster formation among the cell groups. Second, these variables underwent a screening procedure for their variable importance in the projection (VIP) values derived from the OPLS-DA model, ranked the importance of each variable for the classification. Variables with VIP scores≥1 were initially considered statistically significant and observed as the utmost role for differentiating between two groups, while those with VIP scores<1 were eliminated. Thereafter, the integrals of variables with VIP≥1 and the correlation coefficients |r|<=0.05 were selected.

Group means of metabolite integrals were expressed as mean ± std. Variations were calculated through utilizing one way analysis of variance (ANOVA) followed by Dunnett's multiple comparisons test in GraphPad Prism (version 6, GraphPad Software). Significant differences in the mean values were evaluated by Student's *t*-test during acclimating among cell groups. The variables with P<0.05 was considered as statistically significant.

3. Results

3.1 The morphology and proliferation rate of SGC7901 cultured in RPMI1640 were similar to those cultured in DMEM

As the proliferation rate of cells could affect the quantity of detected metabolic products,[24] we firstly determined the morphology and proliferation rates of SGC7901 cells cultured originally in RPMI1640 and DMEM or multiple subcultures in DMEM. No significant differences in morphology were observed among the cell groups (R, R-D 2, R-D 4, R-D 8, D) during the acclimation process (Fig. 1A). Moreover, their proliferation rates were also similar, regardless of the type of culture media and subculture times (Fig. 1B). These results showed that both RPMI1640 and DMEM well fitted for culturing SGC7901 cells, in spite of significantly different levels of some components in the two culture media.

3.2 The metabolic profile of SGC7901 cultured in RPMI1640 was distinctly different from that cultured in DMEM

We performed NMR-based metabolomic analysis to compare the metabolic profiles of SGC7901 cultured in the two different media. Fig. S1 exhibits two typical ^{1}H-NMR spectra of aqueous extracts of SGC7901 originally cultured in RPMI1640 and DMEM, respectively, providing an overview of the metabolic profiles and resonance assignments. Identified metabolites are summarized in Table S2. Both PCA with linear discriminant classification analysis and PLS-DA were conducted on the two cell groups. Obvious discrimination could be observed in their scores plots (Fig. 2A

and 2B) with good cross-validation of permutation tests (999 cycles) (Fig. 2C), demonstrating that the metabolic profiles of SGC7901 originally cultured in RPMI1640 and DMEM were distinctly different, although the differences of their morphology and proliferation ability were not statistically significant. The main discrepant metabolites were extracted from the OPLS-DA loading plot (Fig. 2D), which were potentially the most important factors influencing the metabolic profiles. From the loading plot, 19 discrepant metabolites were identified, including isoleucine, leucine, valine, threonine, alanine, N-acetylgly-coproteins (NAC), proline, taurine, PC, GPC, glycine, tyrosine, phenylalanine, NAD, ATP, glutamate, asparagine, creatine phosphate and choline.

3.3 The metabolic profiles of SGC7901 showed a convergent trend during gradual subculture

To evaluate the effects of culture media on metabolic profiling of SGC7901 cells, we monitored the metabolic profiles of five cell groups (R-D 1, R-D 2, R-D 4, R-D 6, R-D 8) during the gradual acclimation process from RPMI1640 to DMEM. Both PCA and PLS-DA were performed on all the cell samples. The results showed distinct separation and well clustered pattern among these time-related groups in both the PCA scatter plot (Fig. 3A) and PLS-DA scatter plot (data not shown). Apparently changing trends of the metabolic profiles among the cell groups were observed (Fig. 3A). A clear-cut discrimination of the metabolic profile was obtained between the R and D groups. Furthermore, when the culture medium was changed from RPMI1640 to DMEM, the SGC7901 cells showed distinctly different metabolic profile compared with either the

R or D group. However, during gradual subculture, the metabolic profiles of the cells gradually converged toward that of the D group. The more times of subculture the cells underwent, the closer their metabolic profiles to that of the D group. Note that the metabolic profiles of R-D 6 and R-D 8 groups almost converged with that of the D group, indicating the similarities in metabolic profiles among the three groups.

For linear discriminant classification analysis, the classification model has the same covariance matrix for each cluster, only the means vary. The model computes the sample mean of each cluster, and then calculates the empirical covariance by subtracting the sample mean of each cluster from the observations of that cluster. Further linear discriminant analysis based on PCA was performed on all the cell samples. The results exhibited that three clusters were established (Fig. 3A). The R group came into an individual cluster, the R-D 1, R-D 2, R-D 4 groups were gathered into a cluster, and the R-D 6, R-D 8 and D groups were aggregated into another cluster. Samples belonging to the same cluster meant that they shared similar metabolic profiles. Therefore, after six times of subculture during the acclimation process from RPMI1640 to DMEM, the metabolic profiles of SGC7901 had well converged with that originally cultured in DMEM.

In order to identify the dependability of PCA and PLS-DA, both hierarchical clustering analysis and K-means clustering analysis were performed on the binned spectral data by using the website (http://www.metaboanalyst.ca/).[25-27] In the hierarchical cluster analysis, similarity (distance) measure was considered by Pearson's correlation, the clustering algorithms were performed by Ward's linkage

(clustering to minimize the sum of squares of any two clusters). Fig. 3B exhibits the clustering result in the form of a dendrogram. Evidently, the R group forms a separate cluster, the R-D 1, R-D 2, R-D 4 groups belong to another cluster, and the R-D 6, R-D 8 and D groups are clustered together. This result is well consistent with that from the linear discriminant analysis. Furthermore, three clusters were also obtained from the K-means analysis. Table S3 illustrates the members in each cluster, which is in accordance with those analysis results described above. Interestingly, when acclimating SGC7901 cells from DMEM to RPMI1640, the metabolic profiles of the cells also showed a convergent trend toward that of the R group during gradual subculture (Fig. S2).

3.4 Most of the discrepant metabolite levels gradually converged toward those of the D group during gradual subculture

To identify the discrepant metabolites significantly affecting the metabolic profiles of SGC7901 cells during the acclimation process, we performed a careful screening procedure. The screening results are showed in the OPLS-DA loading plot (Fig. 2D) with red and yellow lines to indicate the screened discrepant metabolites. Totally, 19 discrepant metabolites were assigned, including isoleucine, leucine, valine, threonine, alanine, NAC, proline, taurine, PC, GPC, glycine, tyrosine, phenylalanine, NAD, ATP, glutamate, asparagine, creatine phosphate and choline. Furthermore, to identify metabolic pathways that exhibit the main changes in metabolite pool levels, we conducted metabolite set enrichment analysis (MSEA) on the discrepant metabolites by MetaboAnalyst 2.0.[25-27] Fig. S3 overviews the involved metabolic pathways, which

shows that the 19 discrepant metabolites focus mainly on protein biosynthesis, ammonia recycling, methionine metabolism and so on. Then, we performed one-way ANOVA followed by Dunnett's multiple comparisons test to monitor the varied levels of the discrepant metabolites during gradual subculture. The results are presented in Fig. 4B and 4C. The D group was set as control group. These discrepant metabolites in either the R-D 6 group or the R-D 8 group, which showed significantly statistical differences ($p<0.05$) from those in the R group but insignificantly statistical differences ($p \geqslant 0.05$) from those in the D group, were regarded as convergent metabolites. Most of the 19 metabolite levels showed convergent tendencies toward those of the D group. Totally, 15 of the 19 metabolites could be taken as convergent metabolites (Fig. 4B), although some of them displayed varying degrees of fluctuation at the beginning, potentially due to the cellular stress response once coming to a new culture environment. However, four metabolite levels did not converge with those of the D group, including glutamate, asparagine, creatine phosphate and choline (Fig. 4C).

4. Discussion

As a potent approach, cell culture metabolomic analysis is being extensively utilized to assess metabolic pathways and identify characteristic metabolites as well as exploit potential early biomarkers of diseases within living cells. However, culture conditions such as medium composition and supplementation in particular may induce variations in metabolic profiles of cell lines in vitro culture, which could be an obvious obstacle for comparative metabolomic analysis among several types of cell lines with their

own optimum media. Hence, it is difficult to directly compare the metabolic profiles of the cells cultured in different media, and determine whether the transformations of cellular metabolic profiles are related to the changes of biological characteristics of the cells or the differences among the used culture media.

In this context, the present work focused mainly on the effects of culture media on metabolic profiles of the cell lines. We found that the metabolic profile of the human gastric cancer cell line SGC7901 cultured in DMEM was distinctly different from that cultured in RPMI1640, even if the cells showed almost the same cellular morphology and mostly identical proliferation rates. The difference between the two metabolic profiles mostly originated from the differences of the component levels between the two culture media. As two popular commercial culture media for cancer cells, both DMEM and RPMI1640 could be well used for culturing SGC7901 cells as shown in this work. It is expected that the components contained in the culture media could somewhat either up-regulate or down-regulate the levels of endogenous cellular metabolites. For example, compared with RPMI1640, DMEM contains higher levels of some components such as isoleucine, leucine, valine, glycine, tyrosine, phenylalanine and choline (Fig. 4A left, Table S1). Correspondingly, the levels of endogenic metabolites in the D group, including isoleucine, leucine, valine, glycine, tyrosine, phenylalanine and choline, were higher than those in the R group (Fig. 4A right). In addition, RPMI1640 contains glutamate and asparagine, but DMEM does not. As a result, higher levels of glutamate and asparagine were also detected in the R group compared with those in the D group (Fig. 4A, Table S1), which indicated that different

levels of the components contained in culture media could significantly affect cellular metabolic profiles.

The differences of the component levels between the two culture media are mostly amino acids (Table S1). It is well known that amino acids in culture media play central roles both as building blocks of proteins and as intermediates in metabolism. They are crucially required for the syntheses of cellular proteins, the maintenance of cell survival and the integrity of cellular functions. In vitro culture, the levels of amino acids could affect the growth rate and survivability of the cells, which would be reflected on the changes of cellular metabolic profiles.

In this work, the SGC7901 cells originally cultured in RPMI1640 were gradually acclimated in the culture medium of DMEM. The acclimation process did not significantly change cell proliferation capacities. We conducted NMR-based cell culture metabolomic analysis to monitor the varied metabolic profiles of the cells during gradual subculture. Significant variations in cellular metabolic profiles occurred in the initial step when the culture medium was changed from RPMI1640 to DMEM. Then, the cellular metabolic profiles also varied after each time of subculture. Gradually, the metabolic profiles of the cells during the acclimation process converged toward that of the D group, implying that the cells were adapting to a new culture environment. After six times of subculture in DMEM, the metabolic profiles of SGC7901 tended to be nearly stable and almost converged with that of the D group.

Moreover, this work also showed that most of the discrepant metabolite levels gradually converged toward those in the D group with the increasing times of

subculture. The levels of 15 discrepant metabolites were almost convergent with those in the D group after eight times of subculture, including isoleucine, leucine, valine, threonine, alanine, NAC, proline, taurine, PC, GPC, glycine, tyrosine, phenylalanine, NAD and ATP. Note that the amino acids such as isoleucine, leucine, valine, threonine, alanine, proline, glutamate, asparagine, tyrosine and phenylalanine, are usually required for the growth of cells, working as crucial substrates for the pathways of protein biosynthesis and ammonia recycling. The levels of those amino acids gradually converged toward to those in the D group during the acclimation progress, indicative of the integrity of protein biosynthesis and ammonia recycling in cells cultured no matter in DMEM or in RPMI1640.

In vitro culture, some components may exist in the cells as endogenous metabolites although they do not exist in the culture medium. Such endogenous metabolites may be generated from cellular metabolism or transformation of other metabolites. For example, aspargine and glutamate were contained in RPMI1640 but not in DMEM. However, both metabolites were detected in SGC7901 cells originally cultured in RPMI1640 with different concentrations compared with those originally cultured in DMEM. Interestingly, in the acclimating process from RPMI1640 to DMEM, the concentrations of the two metabolites showed convergent tendencies toward those originally cultured in DMEM, although they did not show full convergence after eight times subculture (Fig. 4C). It is well known that, both asparagine and glutamate are not essential amino acids and can be synthesized from central metabolic pathway intermediates in humans without the requirement of taking

from the diet. The precursor to asparagine is oxaloacetate which is converted to aspartate catalyzed by a transaminase enzyme. The enzyme transfers the amino group from glutamate to oxaloacetate, producing alpha-ketoglutarate and aspartate. The enzyme asparagine synthetase produces asparagine, AMP, glutamate, and pyrophosphate from aspartate, glutamine, and ATP. Glutamate exits in cellular mitochondria, lysosome, endoplasmic reticulum and so on, which works as a vital metabolite in ammonia recycling and glutamionlysis. Asparaginase is a hydrolase that catalyzes the conversion of asparagine and glutamine into aspartic acid and glutamic acid, respectively, releasing ammonia in the process. The proliferating cells metabolise glutamine to α-ketoglutarate via the formation of glutamate. In addition, although creatine phosphate was not contained in both culture media, it could be detected in the cells. The level of this metabolite was not fully convergent with that in the D group after eight times of subculture, but showed an evident convergent tendency (Fig. 4C).

Interestingly, the metabolite choline did not converge toward that in the D group. As well known, PC, GPC, choline are crucial metabolites in phospholipid biosynthesis for normal cellular membrane composition and repair. Previous works have observed the elevation of PC, GPC and choline in choline phospholipid metabolism of cancers in different organs.[28-30] In our work, the levels of PC and GPC in the cells during the acclimation process converged with those in the D group, while the level of choline in either the R D-6 or R D-8 group showed a large difference from that in the D group. Choline is one of the most common metabolites in cells with

significant functions in the process of cell proliferation.[31] As an important component of phospholipids, choline is essential for the formation of acetylcholine, and works as a source of methyl groups.[32, 33] During gradual subculture described in this work, choline did not show the similar converging trend adopted by most of the discrepant metabolites. Although the fluctuating choline level also showed a convergent trend, but a large gap was observed between the choline level in the R D-8 group and that in the D group after eight times of subculture (Fig. 4C). Note that the choline level in DMEM is not significantly different from that in RPMI1640 (Fig. 4A left). These results indicate that choline is potentially associated with complicated biological functions. The unique convergent trend of choline might imply that choline could be replaced by other subtracts with similar functions in the culture medium. In addition, the previous work has demonstrated that abnormal choline metabolism is usually associated with oncogenesis and tumor progression.[34] The modulation of enzymes involved in choline metabolism, which is responsible for controlling anabolic and catabolic pathways, may cause increased or decreased levels of choline-containing precursors and breakdown products of membrane phospholipids.[35] The higher choline level and lower PC and GPC levels in the D group compared with those in the R group (Fig. 4B, 4C), potentially indicating the alteration of enzymes activity is associated with choline metabolic pathways. Certainly, further works are required to exploit the underlying mechanism in the future.

Summarily, during the gradual acclimation process from RPMI1640 to DMEM, both the metabolic profiles of the cells and most of the discrepant metabolite levels

converged toward those in the D group with the increasing times of subculture. These results suggest that most of the metabolite level differences between the two media could be almost eliminated through the acclimation. However, several metabolite levels finally did not converge with those in the D group after eight times of subculture. It seems that the differences of the several metabolite levels between the two media could not be mostly eliminated through multiple subcultures, which would cause inaccuracy and unreliability for comparative metabolomic analysis of cell lines.

5. Conclusions

In the present work, we performed NMR-based metabolic profiling of a human gastric cancer cell line SGC7901 in two culture media RPMI1640 and DMEM. We reveal the significant effects of the culture media on cellular metabolic profiles and discrepant metabolite levels. Moreover, we observed distinctly different metabolic profiles of the SGC7901 cells cultured in the two media. Furthermore, we also found that during the gradual acclimation process from RPMI1640 to DMEM, both the metabolic profiles of the cells and most of the discrepant metabolite levels converged toward those of the cells originally cultured in DMEM with the increasing times of subculture. However, we also found several metabolite levels were not convergent with those of the cells cultured originally in DMEM through the acclimation. These results indicate that the effects of the culture media on cellular metabolic profiling must be carefully taken into account for accurately and reliably performing comparative metabolomic analysis of cell lines. This work may be of benefit to cell culture metabolomic analyses which are

being extensively used for mechanistically understanding biological processes of cancer cell metabolism.

Conflicts of interest

The authors did not report any conflict of interest.

Acknowledgements

The work was supported by National Natural Science Foundation of China (Nos. 91129713, 81402064), Science and Technology Project of Xiamen (No. 3502Z20124019)，Natural Science Foundation of Fujian Province (No. 2012D057) , China Postdoctoral Science Foundation (No. 2014M551840) and NFFTBS (No. J1210014).

Notes

† Equal contributions to this work.

* Correspondence should be addressed to Donghai Lin and Caihua Huang, E-mail: dhlin@xmu.edu.cn, E-mail: hch@fjmu.edu.cn; Fax: 86-592-2186078, 86-591-22862201; Tel: 86-592-2186078, 86-591-22862201.

References

1. C. A. Sellick, A. S. Croxford, A. R. Maqsood, G. Stephens, H. V. Westerhoff, R. Goodacre and A. J. Dickson, *Biotechnology and bioengineering*, 2011, 108, 3025-3031.
2. S. Selvarasu, Y. S. Ho, W. P. Chong, N. S. Wong, F. N. Yusufi, Y. Y. Lee, M. G. Yap and D. Y. Lee, *Biotechnology and bioengineering*, 2012, 109, 1415-1429.
3. W. P. Chong, L. T. Goh, S. G. Reddy, F. N. Yusufi, D. Y. Lee, N. S. Wong, C. K. Heng, M. G. Yap and Y. S. Ho, *Rapid communications in mass spectrometry : RCM*, 2009, 23, 3763-3771.
4. A. Ahmad, M. Bayet-Robert and D. Morvan, *PLoS ONE*, 2013, 8, e57971.
5. D. I. Benjamin, B. F. Cravatt and D. K. Nomura, *Cell metabolism*, 2012, 16, 565-577.
6. Q. Bu, Y. Huang, G. Yan, X. Cen and Y. L. Zhao, *Combinatorial chemistry & high throughput screening*, 2012, 15, 266-275.
7. A. Sreekumar, L. M. Poisson, T. M. Rajendiran, A. P. Khan, Q. Cao, J. Yu, B. Laxman, R. Mehra, R. J. Lonigro, Y. Li, M. K. Nyati, A. Ahsan, S. Kalyana-Sundaram, B. Han, X. Cao, J. Byun, G. S. Omenn, D. Ghosh, S. Pennathur, D. C. Alexander, A. Berger, J. R. Shuster, J. T. Wei, S. Varambally, C. Beecher and A. M. Chinnaiyan, *Nature*, 2009, 457, 910-914.
8. I. F. Duarte, A. F. Ladeirinha, I. Lamego, A. M. Gil, L. Carvalho, I. M. Carreira and J. B. Melo, *Molecular pharmaceutics*, 2013, 10, 4242-4251.
9. A. Strigun, F. Noor, A. Pironti, J. Niklas, T. H. Yang and E. Heinzle, *Journal of biotechnology*, 2011, 155, 299-307.
10. M. Cuperlovic-Culf, D. A. Barnett, A. S. Culf and I. Chute, *Drug discovery today*, 2010, 15, 610-621.
11. M. Al-Rubeai and Soo Hean G. Khoo, *Biotechnology and Applied Biochemistry*, 2007, 47, 71.
12. W. Shao, J. Gu, C. Huang, D. Liu, H. Huang, Z. Huang, Z. Lin, W. Yang, K. Liu, D. Lin and T. Ji, *Molecular cancer*, 2014, 13, 197.
13. C. H. Johnson and F. J. Gonzalez, *Journal of cellular physiology*, 2012, 227, 2975-2981.
14. M. Cuperlovic-Culf, D. Ferguson, A. Culf, P. Morin, Jr. and M. Touaibia, *The Journal of biological chemistry*, 2012, 287, 20164-20175.
15. J. L. Wagstaff, R. J. Masterton, J. F. Povey, C. M. Smales and M. J. Howard, *PLoS One*, 2013, 8, e77195.
16. S. E. Mohmad-Saberi, Y. Z. Hashim, M. Mel, A. Amid, R. Ahmad-Raus and V. Packeer-Mohamed, *Cytotechnology*, 2013, 65, 577-586.
17. S. Dietmair, M. P. Hodson, L. E. Quek, N. E. Timmins, P. Chrysanthopoulos, S. S. Jacob, P. Gray and L. K. Nielsen, *Biotechnology and bioengineering*, 2012, 109, 1404-1414.
18. P. Tripathi, P. Kamarajan, B. S. Somashekar, N. MacKinnon, A. M. Chinnaiyan, Y. L. Kapila, T. M. Rajendiran and A. Ramamoorthy, *The international journal of biochemistry & cell biology*, 2012, 44, 1852-1861.
19. C. Hu, Z. Wang, L. Zhai, M. Yang, L. Shan, C. Chai, M. Liu and L. Wang, *Oncology letters*, 2013, 5, 609-612.
20. W. H. Suo, N. Zhang, P. P. Wu, L. Zhao, L. J. Song, W. W. Shen, L. Zheng, J. Tao, X. D. Long and G. H. Fu, *British journal of pharmacology*, 2012, 165, 135-147.
21. Q. Teng, W. Huang, T. W. Collette, D. R. Ekman and C. Tan, *Metabolomics*, 2008, 5, 199-208.
22. F. Dieterle, A. Ross, G. Schlotterbeck and H. Senn, *Analytical chemistry*, 2006, 78, 4281-4290.
23. M. Cuperlovic-Culf, N. Belacel, A. S. Culf, I. C. Chute, R. J. Ouellette, I. W. Burton, T. K.

Karakach and J. A. Walter, *Magnetic resonance in chemistry : MRC*, 2009, 47 Suppl 1, S96-104.

24. K. K. Pasikanti, J. Norasmara, S. Cai, R. Mahendran, K. Esuvaranathan, P. C. Ho and E. C. Chan, *Analytical and bioanalytical chemistry*, 2010, 398, 1285-1293.
25. J. Xia, R. Mandal, I. V. Sinelnikov, D. Broadhurst and D. S. Wishart, *Nucleic acids research*, 2012, 40, W127-133.
26. J. Xia, N. Psychogios, N. Young and D. S. Wishart, *Nucleic acids research*, 2009, 37, W652-W660.
27. J. Xia and D. S. Wishart, *Nature protocols*, 2011, 6, 743-760.
28. M. A. Jacobs, P. B. Barker, P. A. Bottomley, Z. Bhujwalla and D. A. Bluemke, *Journal of magnetic resonance imaging : JMRI*, 2004, 19, 68-75.
29. K. Glunde, E. Ackerstaff, N. Mori, M. A. Jacobs and Z. M. Bhujwalla, *Molecular pharmaceutics*, 2006, 3, 496-506.
30. K. Glunde, C. Jie and Z. M. Bhujwalla, *Cancer research*, 2004, 64, 4270-4276.
31. J. E. Vance and D. E. Vance, *Biochemistry and cell biology = Biochimie et biologie cellulaire*, 2004, 82, 113-128.
32. R. Katz-Brull, D. Seger, D. Rivenson-Segal, E. Rushkin and H. Degani, *Cancer research*, 2002, 62, 1966-1970.
33. H. M. Awwad, J. Geisel and R. Obeid, *Clin Biochem*, 2012, 45, 1548-1553.
34. K. Glunde, Z. M. Bhujwalla and S. M. Ronen, *Nature Reviews Cancer*, 2011, 11, 835-848.
35. D. Gallego-Ortega, T. G. del Pulgar, F. Valdes-Mora, A. Cebrian and J. C. Lacal, *Adv Enzyme Regul*, 2011, 51, 183-194.

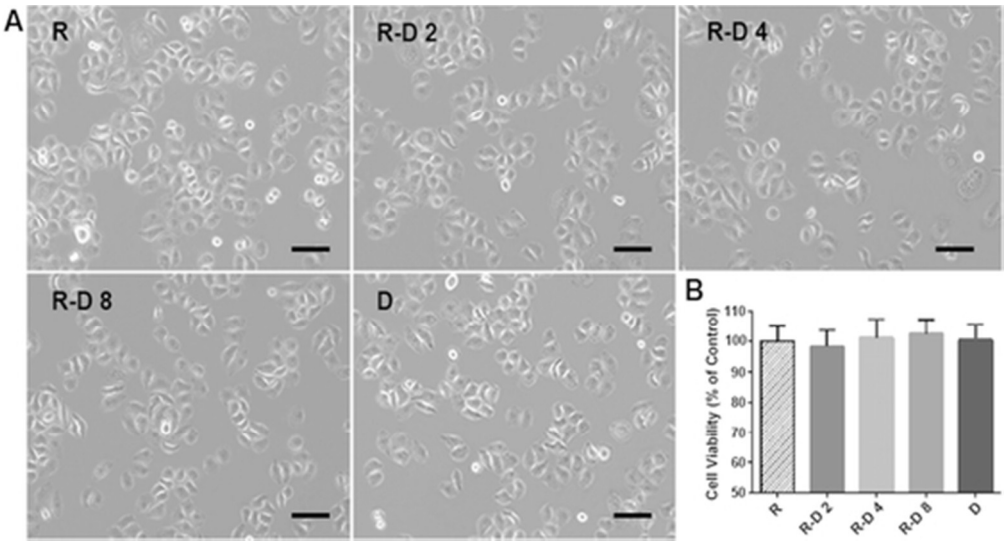

Fig. 1 No significantly difference were observed in (A) cell morphology (scale bar: 100 μm) and proliferation rate ($p>0.05$) on SCG7901 during the acclimation from RPMI1640 (R) to DMEM (D) after 2, 4, 8 times of subculture.
44x23mm (300 x 300 DPI)

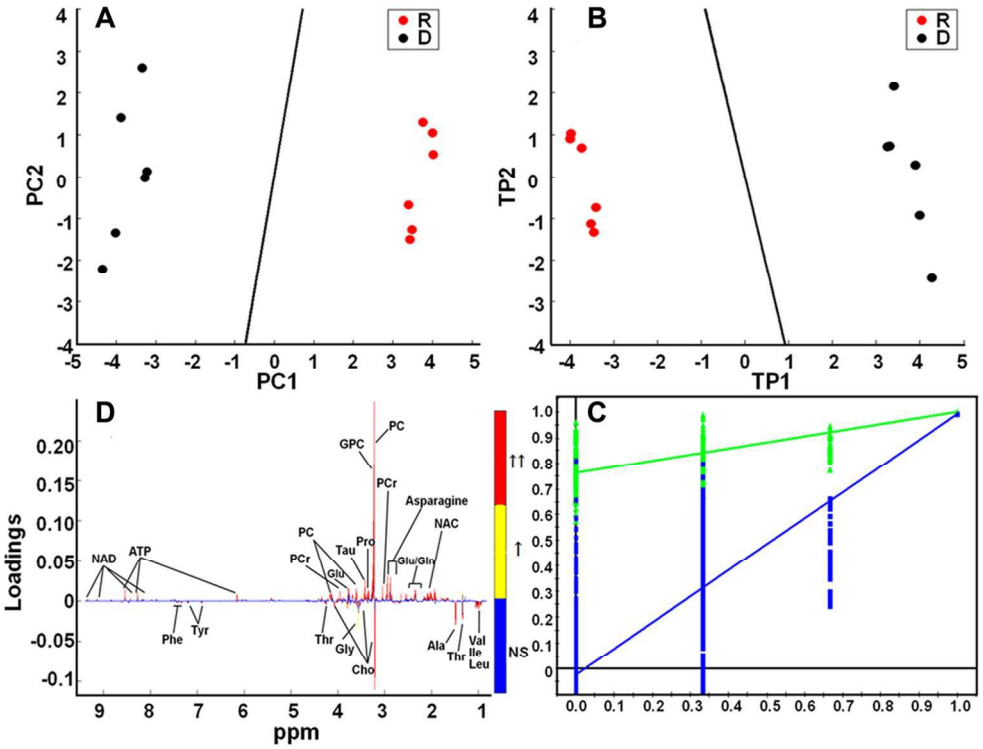

Fig. 2 (A) PCA, (B) PLS-DA scatter plot, (C) PLS-DA cross-validation and (D) OPLS-DA loadings plot of 1H NMR data of aqueous extracts from SGC7901 cells originally cultured in RPMI1640 (R: ●) and DMEM (D: ●).
128x98mm (300 x 300 DPI)

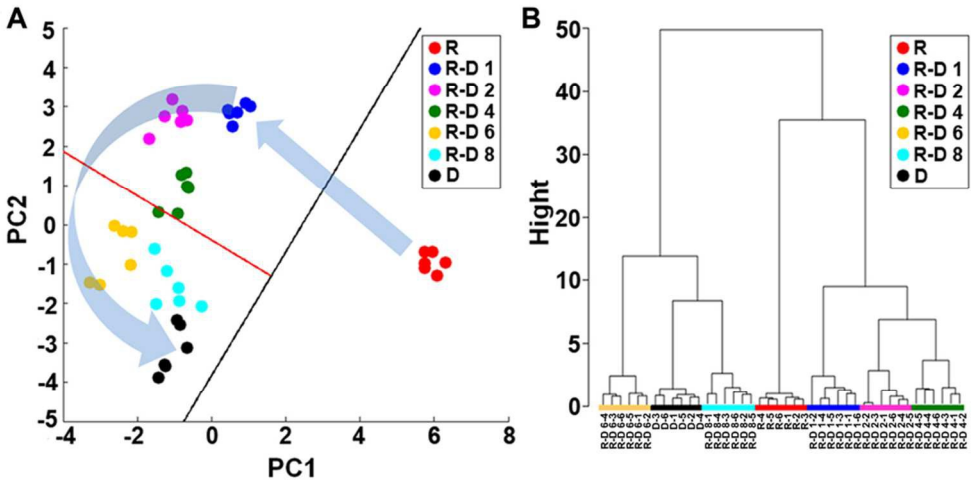

Fig. 3 (A) PCA scatter plot and (B) hierarchical cluster analysis result of 1H NMR data of aqueous extracts from SGC7901 during the gradual acclimation from RPMI1640 to DMEM, which illustrates the changes of metabolic profiles after 1, 2, 4, 6, 8 times of subculture.
85x43mm (300 x 300 DPI)

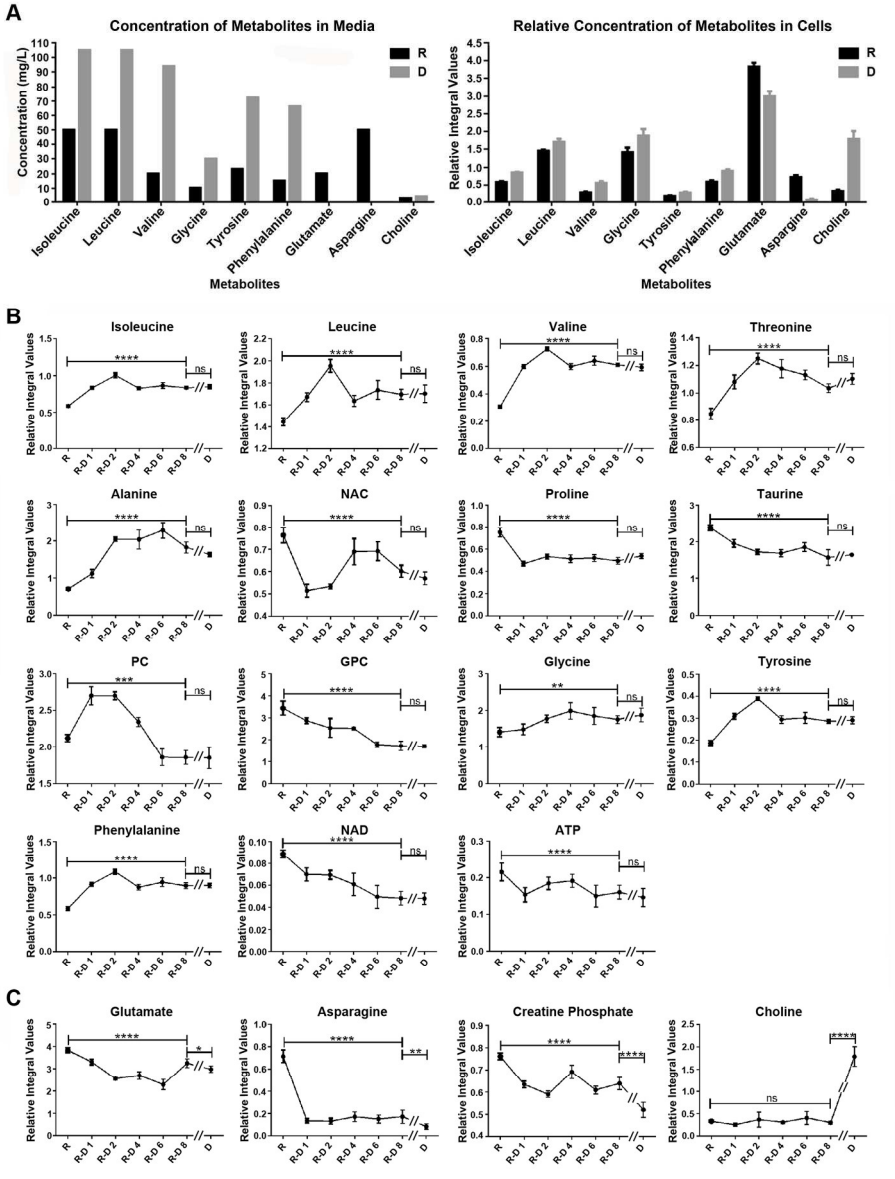

Fig. 4 Univariate analysis of discrepant metabolites in SGC7901 cells. (A) The static concentration of metabolites in culture media (left) and SGC7901 cells cultured in the two media (right). (B, C) The dynamic convergent trends of the discrepant metabolites during the gradual acclimation from RPMI1640 to DMEM. One-way ANOVA followed by Dunnett's multiple comparisons test was performed. In SGC7901 cells after 6 or 8 times of subculture, the levels of some metabolites showed insignificant statistically differences ($p \geq 0.05$) compared with those contained in the cells originally cultured in DMEM, which were regarded as convergent metabolites. (B) Convergent metabolites ($p \geq 0.05$); (C) Not convergent metabolites ($p < 0.05$). ns, $p \geq 0.05$; **, $p < 0.01$; ***, $p < 0.001$; ****, $p < 0.0001$.
217x282mm (300 x 300 DPI)